QRS Morphology-Based EDR Signal–Factors Determining Its Properties

PIOTR PRZYSTUP[1], **ARTUR POLIŃSKI**[2], **AND JERZY WTOREK**[2]

[1]Dynamic Precision Sp. z o. o., 80-172 Gdańsk, Poland
[2]Department of Biomedical Engineering, Faculty of Electronics, Telecommunication and Informatics, Gdańsk University of Technology, 80-233 Gdańsk, Poland

Corresponding author: Artur Poliński (artur.polinski@pg.edu.pl)

ABSTRACT Respiration-induced signals contain a clinically significant information. It could be obtained utilizing both direct and indirect methods. ECG-Derived Respiration (EDR) method is the latter one. However, in this case, two approaches could be distinguished. First one is based on determining changes in the morphology of QRS complexes while the second one is based on the Respiratory Sinus Arrhythmia (RSA) mechanism. The former approach is discussed in the paper. The basic properties of QRS morphology-based EDR signal were evaluated by means of simulations performed using a developed FEM model and appropriate experiments. In effect, basing on changes of the leads' voltages induced by a heart translation or rotation, or by both mechanisms undergoing simultaneously, the sensitivity-like surfaces and the synthetic EDR signals were obtained. A very good agreement of the experimental and simulation results was achieved. The QRS morphology-based signal's properties strongly depend on geometrical relation of the used lead to dominating direction of the heart translation, its rotation, and on personal relation between these two mechanisms. The conclusions presented should be taken into account especially when developing or using QRS morphology-based approach in respiratory monitoring systems.

INDEX TERMS Electrocardiography (ECG), ECG-derived respiration (EDR), respiration monitoring.

I. INTRODUCTION

Respiratory airflow patterns contain clinically useful information, e.g. in stress tests, and sleep studies [1], [2]. The traditional methods of recording respiration patterns require using specially developed techniques such as spirometry, pneumography or body plethysmography [3], [4]. The methods of indirect measurement of respiratory activity are based on respiration-associated biosignals and could be an attractive alternative, e.g. EDR signal is an example of a such approach [5], [6]. In this case, information on respiration is contained in the electrocardiographic signal. However, specially developed processing methods have to be used to gain it. This is because respiration affects both the ECG morphology and the heart rate (HR), i.e. shapes of QRS

The associate editor coordinating the review of this manuscript and approving it for publication was Rajeswari Sundararajan.

complexes and the time distance between them [6]–[9]. The latter mechanism is called Respiratory Sinus Arrhythmia and it is well described in the literature, [10]–[12]. HR increases during inspiration and decreases during expiration. However, it should be underlined that it is not the only mechanism affecting HR [10], [13], [14]. In turn, it is considered that the former mechanism is associated with a respiration-induced rotation of the heart electrical axis [15]. During inspiration, the apex of the heart is faced towards the abdomen, due to an increased filling the lungs with air and simultaneous shift down of the diaphragm. Contrary, the heart apex is faced toward the breast during expiration, because of the diaphragm elevation and the lungs air content reduction [12], [16]. Thus, basing one the ECG morphology it is possible to detect respiration. Several techniques for EDR extraction have been described in the literature. They are based both on a determination of the HR variability and changes of the selected

QRS complexes parameters values. The respiration frequency could be estimated using singular value decomposition [14] or S-transform of HR series [17]. The respiration waveform could be also derived by the extraction of R-wave amplitude modulation with respect to the baseline [13], a calculation of the QRS complex area [16], analyzing the rotation of the electrical axis of the heart [18], as well as by means of more advanced methods, e.g. Kernel Principal Component Analysis [19] or utilizing the wavelet transformation [20].

A careful analysis of the waveforms presented in the papers published elsewhere ([13], [16], [18], [19]) reveals that there is a phase shift between the actual respiration measured e.g. using a nasal sensor and extracted from QRS morphology-based EDR signals. Moreover, it also occurs between EDR signals determined from different ECG leads. The value of the phase shift differed between the studies however, the reason for this was not explained or even discussed. An analysis of the data presented in the literature suggested that this phase could depend on electrode lead configuration and body position [8]. Thus, it could be driven that aside the heart electrical dipole rotation there are also other mechanisms responsible for EDR signal.

A distribution of the electrical potential associated with phenomena undergoing in the heart could be described using the formula proposed by Geselowitz [21]. It follows from this formula that the potential distribution throughout the thorax, and thus on its surface, depends on: 1. the properties of the signal source, 2. spatial distribution of electrical properties of the tissues and organs involved (the thorax and the organs contained in it), and 3. geometrical factors. It could be assumed, without losing the generality of the considerations, that the signal source could be modeled as the moving current dipole. In turn, the electrical properties of all tissues involved could be approximated by electric conductivity in spite of the electrical permittivity of tissues involved, in the considered frequency range i.e. below 1 kHz, achieves very high values. This is a justified approach because imaginary part of complex conductivity is much less than real one. However, it should be noticed that changes of the lungs' conductivity exhibit, among others, dynamics determined by respiration [12], [22].

When considering an equivalent dipole of the cardiac electrical activity it should be noted that, in general, it changes location, moment, and orientation due to depolarization wave propagation throughout the heart [12], [22]. However, if the measurements are done at the same moment of the heart excitation, e.g. at the moment of R-wave appearance, the measured voltage should remain unchanged between any two heartbeats, excluding the cases of an atypical depolarization wave propagation, unless the heart changes its location, or geometry, or orientation, or all of these. The location and orientation of the heart, in relation to the electrodes attached to the anterior chest wall, are subjects to change due to respiration activity [23], [24]. Both variables are multidimensional and are associated with the thorax cage deformation and the diaphragm displacement [25].

A theoretical description of volume source and conductor problem, thus electrocardiography, is detailed in publications [12] and [22]. The bioelectric phenomena are modeled as a quasi-static and linear problem and investigated using, for example, the Finite Element Method (FEM). As a result, it is possible to determine the potential distribution resulting from the electrical activity of the heart, both within and on the surface of the chest [26]–[28]. The accuracy of various approaches is discussed in [29] while the influence of material properties and geometry on the results of the ECG forward simulations is discussed in [30]. A critical discussion about essential aspects of forward problem in electrocardiography could be found in [31].

The aim of the study was to show influence of different mechanisms described below on the EDR signal and to explain the basic properties of EDR, e.g. the phase difference between EDR associated with different ECG leads. In order to achieve it the following sources of EDR signal are considered in the paper: 1. the heart equivalent dipole translation, 2. the heart equivalent dipole rotation, 3. lungs' conductivity changes involved in respiration, and 4. movement of the electrodes caused by the chest movement. Apart from the heart translation, analyzes of the other mechanisms have been presented in many publications [1], [9], [18], [32]. However, the heart displacement has been omitted, until now, in spite of there exist published reports, especially in radiological journals, indicating a relatively large heart translation in response to respiration activity [24]. In the paper the potential distribution at the moment of R-wave of the ECG on the chest wall is simulated. Thus, it enables calculation of the R-wave amplitude for considered electrocardiographic leads. The mathematical model is described by partial differential equation [22], [33]–[35]. The potential is generated by the dipole localized in the heart. Such approach is justified by analysis presented for example in [33], [34], [36]. Basing on that model the measurement properties of EDR signal are explained, especially the phase shift between different ECG leads and the reference signal. The theoretical results were compared with experimental ones obtained using appropriate system of electrocardiographic leads.

II. MATERIALS AND METHODS
The properties of EDR signal extracted from QRS morphology have been examined both experimentally and theoretically. The methods utilized are described in the following subsections.

A. MEASUREMENT STAND AND MEASUREMENTS
The measurements described in this paragraph were performed on a volunteer group consisting of 15 students (all members of the examined group were healthy and declared not having any symptoms of cardiovascular disease or insufficiency). Additionally, the examined students were selected according to the criterion of a similar body posture described by body mass index (BMI). The average value of BMI for the examined group was 28 ± 1.5. All subjects received detailed

information about the study objectives and any potential adverse reactions, and they provided written informed consent to participate in the study. The experimental protocol and the study were approved by the Bioethics Committee at the Regional Medical Chamber in Gdańsk. Each measurement was taken in a standing position and lasted at least 75 s. The examined person was asked to perform three breathe maneuvers (arrest, deep and quiet). The recorded signals were examined by an experienced cardiologist.

The set of signals, containing 3 electrocardiographic leads, acceleration of the selected electrodes, and a nasal air flow, was measured simultaneously. The ECG signals were recorded at a 24-bit resolution. The acceleration was measured in a range $\pm 2g$ using a 3-axis digital accelerometer and respiratory airflow using a nasal mask with built-in thermistor. Both signals were recorded at a 10-bit resolution. The sampling frequency of each signal was set to 250 Hz. A baseline drift from the raw ECG signals was removed using a spline approximation method. Data for this procedure were obtained by calculating an average value of PQ and TP segments for 30 ms and 85 ms, respectively, for each ECG period. The approximated baseline drift signal was determined and then subtracted from the raw ECG signal.

First, the value of the equivalent heart dipole parameters, at the moment of R-wave occurrence, was estimated. An orthogonal system consisting of three leads, i.e. lead 1, 2 and 3, was utilized to achieve this (Fig. 1(a)). A transfer impedance [34] approach was applied to correct components of the dipole, both for the inspiration and the expiration phases. The transfer impedance was calculated using the developed FEM model (described in the next subsection).

Next, EDR signals were determined for three parallel leads, i.e. leads 4, 5 and 6 (Fig. 1(b)). The distance between the two electrodes constituting each lead was approximately 20 cm. Lead 4 consisted of electrodes attached at the midclavicular lines in the 3rd intercostal space. Lead 5 consisted of electrodes attached to the intersections of the midclavicular lines and costal margin of the thoracic cage (at the level of the 8/9 intercostal space). Lead 6 was formed by electrodes attached to the body approximately at the same level as the electrodes
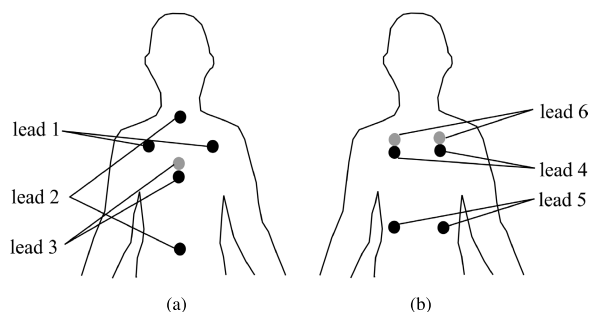
of lead 4. However, the electrodes of lead 6 were placed on the posterior thoracic wall. The EDR was defined as an amplitude of the R-wave in a reference to the baseline of the ECG.

The influence of the heart movement on the EDR signals was estimated by analyzing signals extracted from the ECG recorded by means of leads 4, 5 and 6 (Fig. 1(b)). The localizations and arrangements of the leads was chosen to be sensitive to the heart movement described elsewhere [24], [25].

Additionally, in order to record and to evaluate the range of the chest wall movement, accelerometers were attached to the electrodes of leads 4 and 6. Integrating acceleration signals yielded the velocity of the thorax movement. Next, the integration of the velocity yielded a displacement signal. Thus, information about the electrode movement during the respiration cycle. High pass filter with cutoff frequency equal to 0.01 Hz was applied before each operation of the integration.

B. NUMERICAL SIMULATIONS

The analysis of forward ECG problem can be found in [26] while general considerations are described in [37]. According to above mentioned papers and [35] an electric potential field in the thorax could be calculated using the partial differential equation

$$\nabla \cdot (\sigma \nabla \psi) = -I_{SV} \qquad (1)$$

where

$$I_{SV} = -\nabla \cdot J_h \qquad (2)$$

and J_h denotes the cardiac source. Additionally, the current density normal to the thorax surface, S, has to fulfill a boundary condition

$$\frac{\partial \psi}{\partial n} = 0 \quad \text{on } S \qquad (3)$$

where n is a unit vector normal to S. The potential distribution associated with electrical heart activity was modeled using an equivalent dipole approach [12], [22], [34], [35]. The value of the dipole moment was equal to $2.0 \cdot 10^{-5}$ Am. This was in agreement with the data available elsewhere [33], [38]. The initial, reference values of azimuth and elevation angles were 150° and 135°, respectively. They are referred to the coordination system presented in the Fig. 2. FEM model of the thorax was developed (Fig. 2). It contained heart filled with blood, lungs, and thoracic wall, each of different and appropriate conductivity, while the remaining organs located below the diaphragm were included as an electrically uniform tissue.

The model was developed based on images obtained by means of Computer Tomography (CT) measurements. The CT data were segmented and exported to *.stl files using Slicer software. In order to reduce the mesh complexity, quadratic edge collapse decimation was performed, together with Laplacian smoothing. Both operations were done using the Meshlab software. The final model contained over 110,000 tetrahedral elements. The x-coordinate was oriented
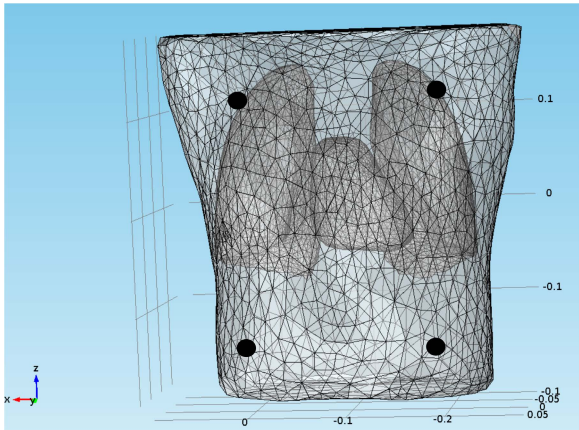

FIGURE 1. The electrocardiographic leads used in the study: (a) orthogonal ones used for determining equivalent heart dipole, and (b) parallel ones, including anterior (leads 4 and 5) and posterior (lead 6), for evaluating properties of EDR signals.

FIGURE 2. FEM model of the torso with lungs made visible and locations of electrodes (lead 4 and 5), compare to Figure 1.

TABLE 1. The dipole parameters derived from measurements.

	Dipole length [Am] 10^{-5}	Azimuth [°]	Elevation [°]
Expiration	2.21 ± 0.55	147 ± 6.8	137 ± 7.4
Inspiration	1.96 ± 0.52	152 ± 8.6	134 ± 9.2

distribution. All changes were defined in a reference to the midrespiration state. Then, the calculated voltages of leads 4 and 5 were determined and were distributed uniformly with arbitrary interval along the time axis. Next, an interpolation procedure, using spline method, was applied in order to achieve a time course of respiration patterns, i.e. the synthetic EDR signals.

In all FEM simulations the partial differential equation with boundary condition, i.e. equations (1)-(3) were solved. For each step of simulation (i.e. the heart dipole location and direction, the lungs' conductivity) the forward problem was solved. FEM simulations were performed using Comsol® software.

III. RESULTS
The measurements and simulation results are presented in this section. The former, are presented in the form of recorded signals, i.e. air flow, electrodes movement or EDR signals obtained using leads 4, 5 and 6. The latter, i.e. the simulation results are presented using two approaches. The first relies on presentation of the voltage change (sensitivity-like presentation) for the certain lead as a function of two selected variables while the third one is treated as the three-valued parameter. The second is based on a synthetic respiration pattern presentation. The value of the variable or variables responsible for the leads' voltage changes have been so taken as to achieve the leads' voltages comparable to these measured in real cases.

A. RESULTS OF EXPERIMENTS
The first step was to determine the dipole parameters for numerical simulations. The components of the dipole moment, in x, y, and z directions for expiration and inspiration phases have been calculated for each person. Based on that, the dipole orientation, i.e. the azimuth and the inclination angles, were estimated. The dipole parameters (mean±sd) were estimated both for expiration and inspiration (Tabel 1).

The influence of respiration on the electrodes movement was determined for leads 4 and 6. In general, the chest movement associated with breathing is a complicated function of many variables, e.g., depth of breath, measurement site, sex, etc. To minimize an influence of above-mentioned variables on the recorded ECG, the upper part of the thorax was selected for localization of two leads, i.e. leads 4 and 6 [46]. The electrodes' movement was measured by means of accelerometers attached to two electrodes, the posterior and anterior ones. Simultaneously a reference signal, i.e. airflow using a thermistor mounted in the nasal mask, was recorded (Fig. 3).
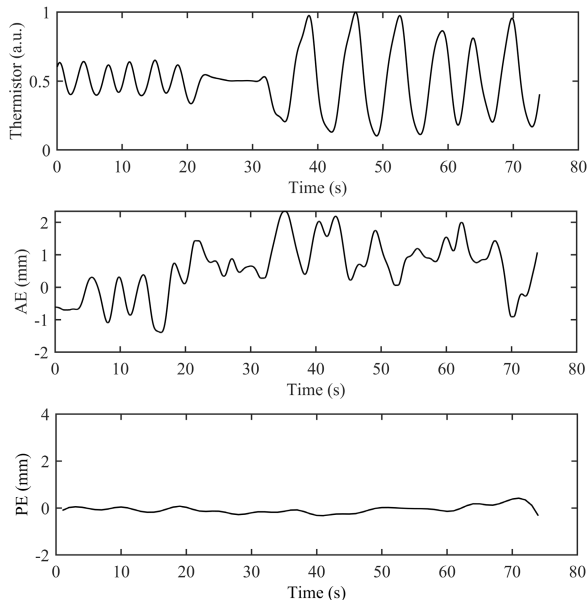
from left to right shoulder (frontal plane), the y-coordinate from back to front (sagittal plane) and the z-coordinate from bottom to top. The center of the heart base, i.e. $(-0.1, -0.03, 0)$, was set as the position corresponding to a midrespiration state.

The conductivity value assigned to each tissue included in the model was selected according to the frequency spectrum of the ECG. Thus, the conductivity of the heart muscle, the thoracic wall, the blood and the abdominal part of the body (the part below the diaphragm) were, respectively, equal to 0.2 S/m, 0.1 S/m, 0.5 S/m, and 0.1 S/m [39]–[43]. In the case of the lungs' conductivity, aside from its basal value equal to 0.05 S/m, also the respiration-induced changes were estimated. To estimate the range of these changes, an approach based on a relationship describing the conductivity of a mixture was adopted [39], [44]. In result, the lungs' conductivity changes due to respiration activity were ± 0.0025 S/m [39]–[41], [45].

Above values corresponded to the midrespiration phase in simulations. However, in the numerical experiments presented in the next sections, much higher changes of the lungs' conductivity were also examined. It was assumed that the equivalent dipole of the heart ventricles' depolarization, at the moment of the R-wave, was located in the center of the heart base and moved simultaneously with it in the numerical experiments [12], [22]. Thus, the geometrical relation of the dipole origin to the heart was preserved during its movement. The dipole translation was assumed to be ± 10 mm from the midrespiration position in each of examined direction, i.e. x, y, and z [23], [24]. Similarly, the dipole rotation was modeled assuming a change of azimuth and elevation angles in the range up to $\pm 30°$ in different numerical experiments.

When calculating the EDR signals patterns and their properties, for one inspiration-expiration cycle, the voltages of three leads, i.e. 4, 5, and 6, were considered (Fig. 1(b)). The voltages were calculated for seven slightly modified FEM models each corresponding to different phase of the cycle. Modifications relied on changes in the position and direction of the heart dipole and as well as on spatial conductivity

FIGURE 3. Air flow signal (upper trace) and associated movement of anterior (AE) and posterior (PE) electrodes measured by accelerometers. Signals were recorded during quiet (0÷20), arrest (20÷30) and deep (30÷75) breath manoeuvres.
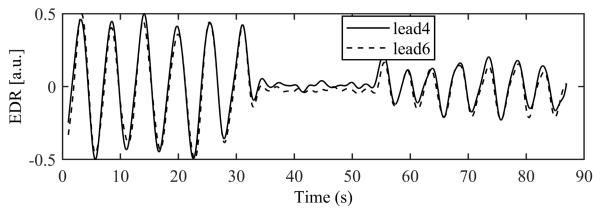

FIGURE 4. The EDR signals extracted from the electrocardiograms recorded at the anterior and the posterior part of the thorax using leads 4 and 6. The EDR signals were normalized and mean values were removed. The presented signals were recorded during deep (0÷35), arrest (35÷55) and quiet (55÷90) breath manoeuvres.
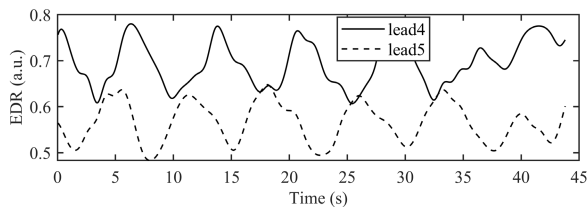

FIGURE 5. The EDR signals extracted from the electrocardiograms recorded by means of leads 4 and 5.

The EDR signals were extracted from the ECG recorded by means of leads 4 and 6 during different respiration maneuvers (example in Fig. 4).

Two EDR signals were also calculated based on the electrocardiograms recorded using leads 4 and 5 (example in Fig. 5).

B. SIMULATION RESULTS

A set of simulations assuming a different complexity of the dipole movement and spatial conductivity distributions was performed.
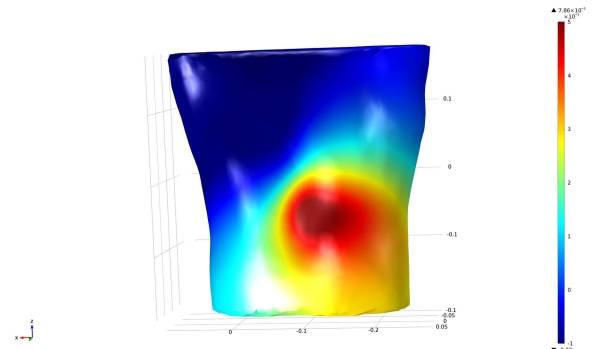

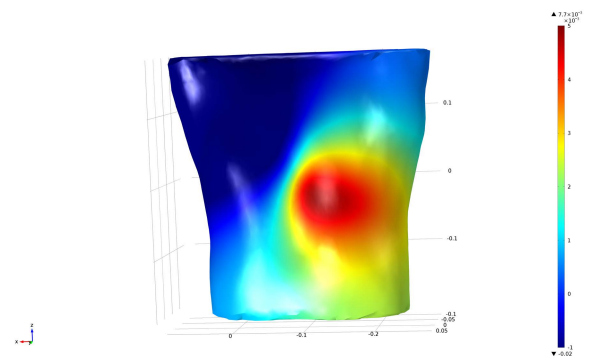**FIGURE 6.** The potential distribution on the thorax for maximal inspiration phase.

FIGURE 7. The potential distribution on the thorax for maximal expiration phase.
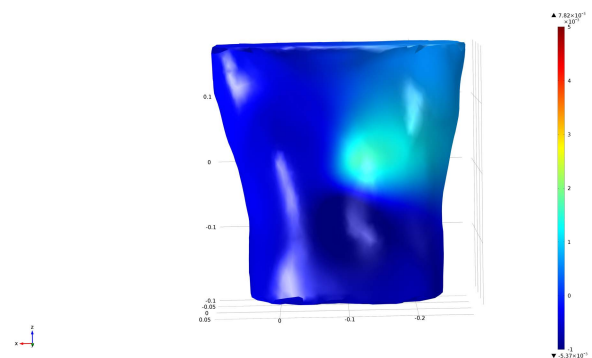

FIGURE 8. The difference between potential distribution on the thorax between maximal expiration and inspiration.

Examples of potential distributions on the thorax for two dipole locations (inspiration and expiration) and the difference between them are presented in Figs. 6-8.

The impact of the selected variable or set of variables on a potential difference (dV) between electrodes of the lead was calculated and referenced to the value V_0, where V_0 was the potential difference for a midrespiration phase. Thus, the relative voltage dV was defined as follows:

$$dV = \frac{V - V_0}{V_0} \cdot 100\% \qquad (4)$$

First, the impact of the heart translation (thus also the equivalent dipole) in different directions on the leads' voltage
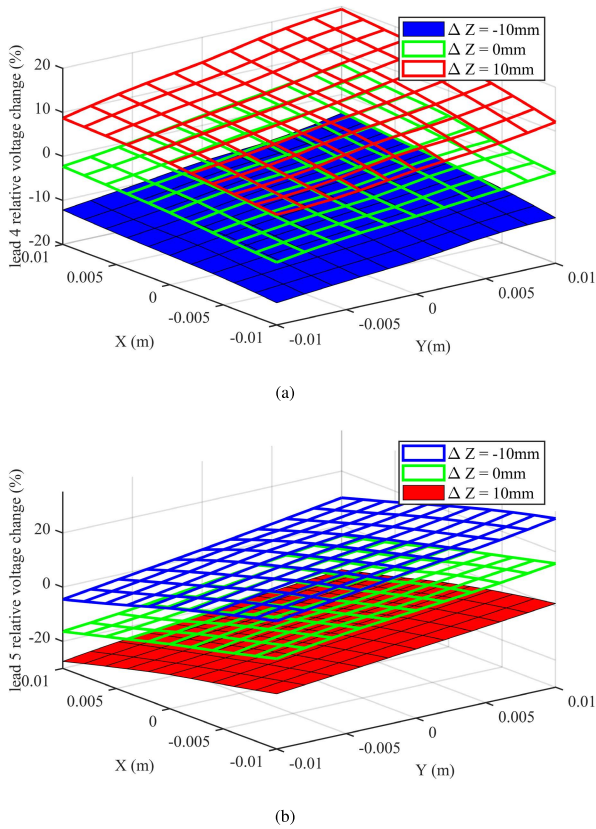
(a)

(b)

FIGURE 9. An influence of the heart dipole translation from its basal position on voltages of (a) lead 4 and (b) lead 5.

(a)

(b)

FIGURE 10. An influence of the heart dipole rotation and simultaneous translation along x-coordinate from its basal position on voltages of (a) lead 4 and (b) lead 5.

was examined (Fig. 9). To show the influence of the dipole translation in all three directions on the leads' voltage, the data are presented as a two variable graph (x and y) while the third one (z) is a three-valued parameter (Fig. 9). In fact, the calculations were performed for all coordinates with the same discretization.

The results obtained for other combinations of variables, i.e. x and z while y was the parameter or y and z while x was the parameter, were very similar to these presented in Fig. 9. Almost planar and parallel surfaces were obtained, however, with a slightly different distance between them and the slopes.

Next, the azimuthal and elevation angles were assumed to be continuous variables while translations along a certain coordinate were assumed as the parameter (Figs. 10 and 11). The changes of both considered angles were assumed to be much larger than in actual cases. Basing on this approach it is possible to estimate properties of the method for a wider parameters changes or different reference point. The lungs' conductivity changes, in spite of using its relatively large range, i.e. ±0.01 S/m, had a minor impact on the leads' voltages (Fig. 12). Additionally, they influenced voltages of leads 4 and 5 almost in the same manner.

Next, synthetic respiratory signals from the data obtained using the simulation studies using the FEM model are presented. The respiration patterns presented were obtained, by calculating the leads' voltages for seven sets of all
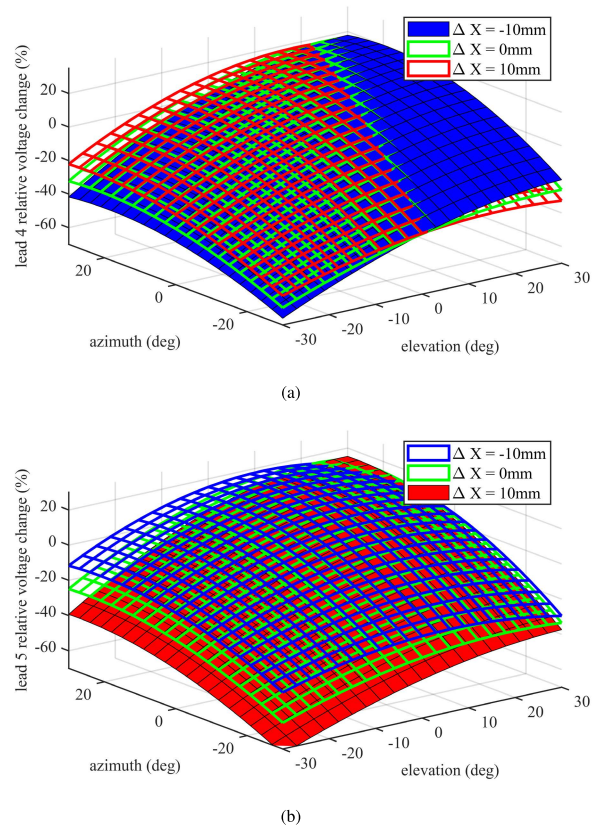
considered parameters. First, the synthetic respiration pattern assuming only the translations of the heart and dipole along the z-coordinate was constructed (Fig. 13). It should be underlined that the respiration patterns, for leads 4 and 5, obtained are out of phase. Similar respiration patterns could be developed for the translation along the x or y coordinates or along any arbitrary direction.

Again, assuming a one-variable mechanism of the EDR signal, in turn based on the azimuthal angle changes, the resulting EDR signals for the leads 4 and 5 are in phase (Fig. 14).

Similarly, the impact of the elevation angle changes results in in-phase signals for leads 4 and 5 (Fig. 15). However, the relation between the signals' amplitudes is different.

The lungs' conductivity changes involved in respiration also influence the leads' voltage (Fig. 16). Again, the resulting signals, for the leads considered, are in-phase and are of significantly different amplitudes. In spite of conductivity changes being very large in comparison to physiological ones, the resulting signals are rather small when comparing to other mechanisms. When including all mechanisms however, assuming actual relations between them, the resulting leads signals exhibit an out-of-phase relationship between them (Fig. 17). The magnitude of each mechanism total change was equally divided between the successive steps (FEM models).
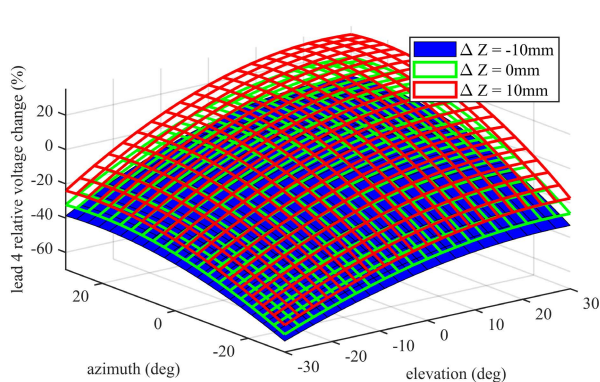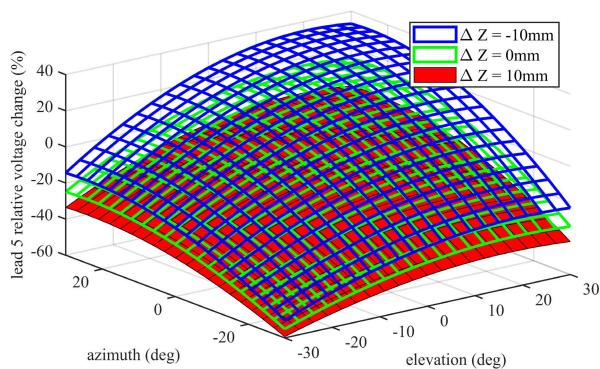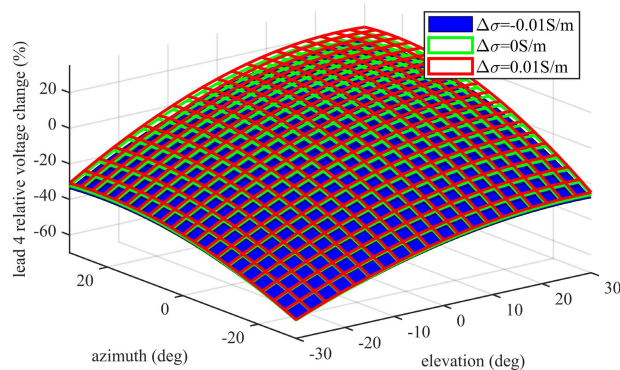
FIGURE 11. An influence of the heart dipole rotation and simultaneous translation along z-coordinate from its basal position on voltage of (a) lead 4 and (b) lead 5.

FIGURE 12. An influence of the heart dipole rotation from its basal position and simultaneous the lungs' conductivity change from its basal value on voltage of (a) lead 4 and (b) lead 5.
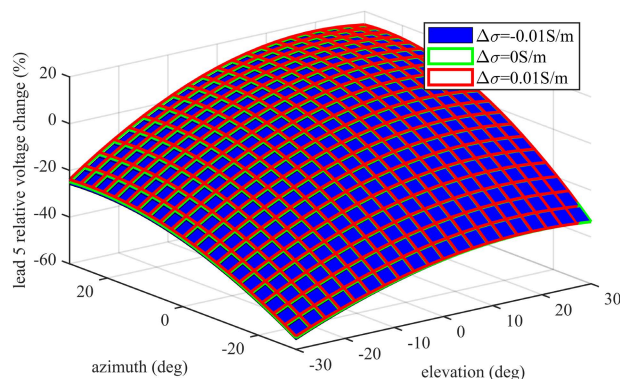
The different approach resulted in similar respiration patterns (Fig. 18). It was assumed that at the beginning of the heart movement, starting from inspiration phase, only the translation was present. The rest mechanisms were included when the heart achieved half of the total translation distance (midrespiration phase). In contrast to the previous examination, aside translation, the total changes of other mechanisms were achieved in lower number of steps.

IV. DISCUSSION

The EDR algorithms based on QRS morphology are considered more useful and reliable in determining respiration activity than those based on HR variability, [5], [6]. This is because the modulation of HR by respiration is sometimes lost or embedded in other parasympathetic interactions [10], [13], [14]. This is the main reason to study the measurement properties of the approach based on QRS morphology. Analysis of the relationship describing the electric potential distribution in a nonuniform and bounded volume conductor allows for deduction of the possible mechanisms determining the value of the ECG voltage measured using a certain lead, [21], [34], [35], [47]. In general, the factors determining the ECG voltage could be both geometrical and/or material dependent. The former includes the configuration of the electrode lead, its localization in reference to the heart,

FIGURE 13. A simulated time courses of respiration resulting from the heart dipole translations along the z-coordinate. The translation was equal to ±4 mm around the midrespiration position.

FIGURE 14. A simulated time courses of respiration patterns resulting from the heart dipole rotation. The rotation was limited to azimuth angle changes. Its total change around the basal value was ±5°.

the shape of the thorax and organs modeled, etc., while the latter includes the electrical properties of the tissues, both active and passive, participating in the measurement.
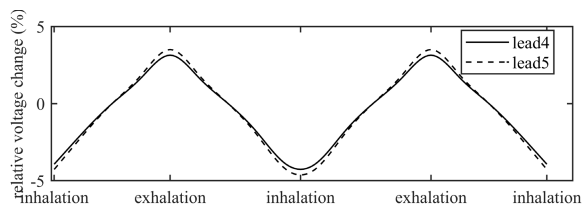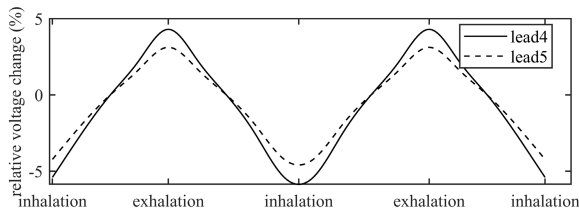
FIGURE 15. A simulated time courses of respiration patterns resulting from the heart dipole rotation however, limited to elevation angle changes. Its total change around the basal value was ±3°.
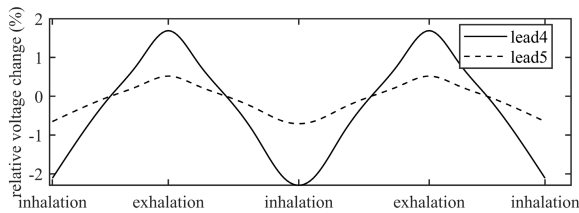

FIGURE 16. A simulated time courses of respiration patterns resulting from the lungs' conductivity change. The conductivity change around the basal value was ±0.008 S/m.

As a result, the four respiration-induced mechanisms described in the Introduction are considered in the paper. To examine the influence each of the above-mentioned mechanisms on the EDR signal, experimental and numerical studies were performed.

The measurements were performed on volunteers with similar value of BMI. It was assumed, to some extent, that such limitation led to a similar character of the heart respiration-induced movement. This assumption was somehow supported by a low interpersonal variation of the equivalent dipole parameters (Table 1). The dipole parameters were determined experimentally from ECG measurements and supported by literature data, [33], [38]. The obtained dipole components were corrected using the method based on transfer impedance approach as proposed by Geselowitz [34]. However, it should be underlined that the utilized approach was of limited accuracy. Among others, it follows from a small number of measurement channels used and an assumption on a fixed position of the dipole. There was a relatively significant difference between the dipole moment obtained for the expiration and inspiration phases (Table 1). The average value of the dipole moment was
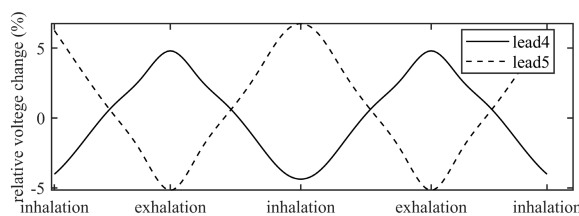

FIGURE 17. A simulated respiration patterns assuming the simultaneous changes of translation along z-coordinate, rotation (azimuth and elevation) and the lungs' conductivity. They were, respectively, equal to ±4 mm, ±1°, ±2°, and ±0.0025 S/m.
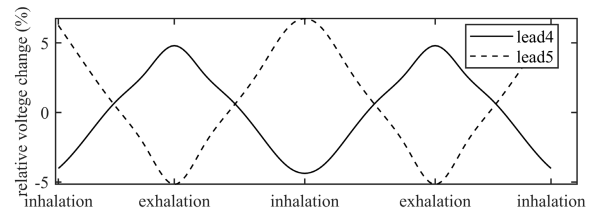

FIGURE 18. A simulated respiration pattern assuming a sequential inclusion of the considered mechanisms. At the beginning, the heart was translated along the z-coordinate and when arriving at half of the assumed translation the rest of considered mechanisms were included. They were described by exactly the same amplitudes as in previous case (Fig. 17).

utilized in the simulation studies. Nevertheless, in spite of the above-mentioned limitations, the dipole parameters used in the simulation study produced potential distributions and lead voltages comparable to the actual ones. On the other hand, the problem considered is a linear one, thus an inaccurate value of the dipole moment does not influence the interpretation of the results obtained. Especially, if their relative values are considered. An analysis of the accelerometric and airflow signals showed that there was very low correlation between them. There was insufficient evidence to conclude that there was a significant relationship between the airflow and accelerometric signals. This applies to both the signals recorded on the anterior and posterior parts of the upper chest. However, according to the data, the posterior electrodes (lead 6) were rather still in comparison to the anterior ones (lead 4) (Fig. 3). A significant independence of the lead 4 voltage on the electrodes' movement could be explained by the fact that they move simultaneously and in the same manner [32], [46]. Additionally, this property explanation is supported by a very high and expected similarity of the EDR signals based on the electrocardiograms recorded by means of leads 4 and 6. Assuming that the electrodes' movement is an essential mechanism, there should be a much higher difference between these signals. Thus, the electrodes' respiration-induced movement could be omitted, as its contribution to the EDR, when comparing to other mechanisms is marginal.

The three parallel leads were, both in the experiments and in the simulations used to determine the basic properties of the EDR signal and associated mechanisms. The leads' configuration and localizations were chosen according to the anticipated measurement properties following from the spatial sensitivity distribution [22]. Let's note that the dipole angle changes should create three in-phase EDR signals for these leads. In turn, when the dipole is located between two leads, the displacement towards one of them will cause a simultaneous decrease of one and increase of the other signal. In other words, these signals will be in opposite phases. Thus, a translation of the dipole along the caudal-cranial direction produces out-of-phase EDR signals for leads 4 and 5 while in-phase for leads 4 and 6. Similarly, a movement in the posterior-anterior direction produces out-of-phase EDR signals for leads 4 and 6. When considering leads 4 and 6, there is almost no difference in the signals (Fig. 4). It could be

concluded that the small differences are acceptable. A close inspection of the results presented in Fig. 5 shows a significant difference in the phase between leads 4 and 5 signals. This feature could be easily explained by equivalent dipole translation along the z-coordinate. In contrast, it could be not explained by the dipole rotation.

There are different approaches enabling calculation of the lead voltage. The method used in the paper is not restricted to certain electrode configuration as it delivers a potential distribution overall the thoracic surface. Assuming a measurement lead configuration, i.e. electrodes' localization, the results obtained could be evaluated using approach proposed in [32]. The lead voltage V_l is given by the relationship

$$V_l = H \cdot l \tag{5}$$

where H is the heart vector (dipole) and l is a lead field associated with a given lead (electrodes localization on the thorax) and the dot means a scalar product. Assuming that the H vector is, at each period of the heart excitation, estimated at the same moment of QRS complex, i.e. R-wave in the considered case, the H vector preserves its length while its direction and position in the thorax are subject to changes. Assuming that the vector H is translated and simultaneously changes its direction in the lead field l the resulting lead voltage change could be evaluated from the relationship

$$\Delta V_l = l \cdot \Delta H + H \cdot \Delta l + \Delta H \cdot \Delta l \tag{6}$$

where ΔH is the heart vector change and Δl lead field vector change. The lead vector change, Δl, follows from the fact that to each point of the thorax a different value of l is assigned for the configuration of leads used. It is in contrary to the assumptions accepted in [15] and widely cited in the "EDR" literature. It is assumed that the only mechanism determining the lead voltage is the heart vector rotation (changes of direction). It is equivalent to omission of the second and the third components of the formula (6).

Due to the conclusions from the experimental studies and above discussed reasons, the external geometry of FEM model was assumed to be fixed, i.e. independent of respiration activity. This assumption was justified, at least, for leads 4 and 6. However, the assumed model complexity and associated spatial conductivity distribution is not only one of simplification. Another one followed from the utilized signal source model, i.e. the equivalent dipole approach. In fact, the depolarization wave propagation along the ventricle muscle approach could be a more appropriate. It would allow a more advanced simulation studies to be performed. Nevertheless, our approach is justified as it is noted in [36] that "it leads to a surprisingly good results". Moreover, taking into account that the examined group of volunteers in experimental studies was almost "uniform" and healthy an approximation utilized in the study could be considered as an appropriate one.

According to our knowledge, rotation of the equivalent heart dipole is considered a dominating and responsible mechanism for the QRS morphology-based EDR signal [5], [15]. A basic drawback of this explanation is the impossibility

of interpreting the EDR signal in terms of its phase in reference to a direct recording of airflow [1], [5]. Moreover, the phase difference between these signals depends on the lead configuration [8], [16]. On the other hand, there are studies supporting the hypothesis that the heart movement induced by respiration activity is more complex than rotation only, [23]–[25]. Aside from the heart rotation, there is also its translation (in 3D space) and deformation. According to the solid angle theory, an influence of ventricles deformation on the lead voltage could be omitted, at the first approach [22], assuming that the depolarization wave propagation remains unchanged by ventricles deformation. In turn, the heart translation trajectory, according to the data published, is very often personal [24]. However, the component along the z-coordinate seems to be the dominating one. According to data available in the literature [23]–[25] the average value of translation along z axis is 4.9 mm while the average change of elevation angle is only $1.5° \pm 0.9°$. In turn, the average change in azimuthal angle is $1.2° \pm 1.3°$. Of course these data are valid only for the examined group of patients. In spite of this limitation, the translation along the selected directions was examined (Fig. 9). The displacement in the direction of the z-coordinate leads to an opposite change of the voltage for leads 4 and 5 (the same color is used to mark positive or negative displacement through all figures 9-12). It explains the opposite phase of EDR signals property. It is known from electrocardiology [22] that the signal character depends on the relation between the directions of the heart movement in reference to the lead used in the measurements. Similar drawings could be developed for other combinations of x, y and z as variables and the parameter. However, the translations along x or y directions are described by the sensitivity of the same sign for the leads considered. Thus, they are in phase (these figures are not presented in the paper however, this property could be deduced from Fig. 9).

Interesting results were also obtained when combining rotation with translation along the selected direction (Figs. 10 and 11). It should be noted that along the intersection of the presented surfaces (Fig. 10) the sensitivity to changes in displacement in the x-coordinate (left to right axis) is zero. Moreover, on one side of the intersection curve, the sensitivity is positive while on another, negative. The intersection curves are different and located differently for the examined leads (compare Fig. 10(a) and 10(b)). This means that the same change in displacement along the x-coordinate, depending on the value of the azimuth and elevation angles, could lead to an increase or decrease in the lead voltage. It is equivalent to the statement that the translation "deforms" rotation-based surfaces of the lead voltage. Contrary to the results shown in Fig. 10, the surfaces for different translations along the z-coordinate do not intersect and they are relatively distant each from other (Fig. 11). This is in spite of the fact that the calculations were performed for an identical range of elevation and azimuth angles in both cases (Figs. 10 and 11). Similarly to the results presented in Fig. 9, the relative changes of voltage for leads 4 and 5 are opposite.

This figure also enables (more clearly than using Fig. 10) the result to be forecast from the model assuming only changes of elevation and azimuth angles, i.e. when a rotation-based-only model of the EDR signal is assumed. Just compare the green colored surfaces for the two leads considered. Please note that the voltage change, resulting from the change of only one angle resembles a segment of a sinusoidal function independent of the angle considered. A similar prediction could be made using data obtained for a rotation and conductivity changes-based model (Fig. 12). The lungs' respiration-induced conductivity changes result mainly from the different air content in the lung tissue [39], [45], [48]. A short term changes are considered only. They were estimated using a mixture theory approach [39], [44]. The contribution of this mechanism to the leads' voltages was linearized assuming that the midrespiration value of lungs' tissue conductivity was exactly equal to the mean one. However, it does not change the generality of the results obtained. One can expect only a slight modification of the result. Summarizing, the influence of conductivity on the rotation-induced voltage is minimal however, the lead 4 seems to be slightly more sensitive to the lungs' conductivity changes than lead 5. This result seems to be reasonable.

The synthetic respiration-induced patterns created by different mechanisms are presented in Figs. 13-18. They were obtained by choosing the range of particular variable changes to obtain the appropriate amplitude of the patterns, comparable to the actual ones. Thus, in some cases, these values are not necessarily physiological ones. Assuming only one mechanism of the EDR signal that is based on the translation of the equivalent dipole along the z-coordinate results in out-of-phase signals for leads 4 and 5 (Fig. 13). This property is already discussed in the paragraph evaluating the experimental results. According to the data presented in Fig. 10, translation along x-coordinate could also lead to in-phase or out-of-phase signals when considering leads 4 and 5. It depends on the range of variable changes and the midrespiration value of the elevation and azimuth angles. However, the translation along the x and y coordinates leads to in-phase signals for the midrespiration values considered in the paper and the assumed range of changes. Changes of elevation or azimuth angles only leads to in-phase signals (Figs. 14 and 15). This property of the signals is also supported by the data presented in Figs. 10-12. At the first approach, the contribution of the elevation or azimuth angles changes to the leads' voltage depend on the dipole projection on the lead direction [22]. Simplifying, the lead direction is determined by a line connecting the electrodes of the lead (see the explanation of the ECG voltages for the Einthoven triangle [22]). Thus, for the parallel leads, the signals should be in-phase, assuming an azimuth-elevation changes model.

In-phase synthetic signals for leads 4 and 5 were obtained for the lungs' respiration-induced conductivity changes (Fig. 16). Unfortunately, we were not able to support numerical results by performing *in vivo* experiments. Therefore, the influence of the lungs' conductivity change during respiration

(different content of air) on the EDR signal was only examined using the FEM model.

Performing the calculations for all mechanisms included in the model led to out-of-phase respiratory patterns (Figs. 17 and 18). The patterns were calculated using 7 sets of data containing all considered mechanisms. The changes range of individual variables were, respectively: translation (0, 0, ±4) mm, elevation ±2°, azimuth ±1°, and change in the lungs' conductivity ±0.0025 S/m. Two approaches were adopted. The first relied on the inclusion of all mechanisms (translation, rotation and change in conductivity) simultaneously for each step, i.e. typical values of individual variables were evenly divided into 7 consecutive steps making up one breathing maneuver (i.e. inspiration or expiration) [23]. In the second one, the heart movement was divided into two successive and equal time segments. During the first one, only the translation along the z-coordinate was performed. Then, all types of the movement and lungs' conductivity changes were included. However, each step during this period was characterized by larger value changes of individual variables to finish the movement at the same place in space as was achieved in the first case. Thus, in both cases, the total changes of variables were identical between inspiration and expiration phases of respiration. The purpose of this experiment was to show that various and realistic scenarios of the heart movement minimally modifies the calculated EDR patterns. Moreover, the patterns obtained for both simulations preserved the out-of-phase property. It should be underlined that a significant modification of the variables describing the heart's movement, e.g. a decrease in the translation component describing the movement along the z-coordinate and simultaneously a significant increase component describing the movement along the x-coordinate could lead to a totally different result. The adequacy of the proposed model seems to be supported by the fact that the calculated respiration patterns are almost identical to those obtained from the measurements (Fig. 5).

Taking into account the results of the study, a few comments on the model adequacy are necessary. First, the relation between the electrical and the geometrical heart axes seems to be crucial. It is reported that respiration-induced changes of electrical heart axes are much bigger than considered in the study [12], [22], [49]. However, it should be underlined that there is not a clear relationship between the geometrical and electrical heart axes [50]. This could follow from many reasons. First, most of the data presented in the literature have been collected assuming only a rotation-based model. There is a lack of literature reporting a serious examination of heart translation impact on the electrical heart axis. Second, it seems that a basic impact on the electrical heart axis orientation has repeatability of the depolarization wave propagation throughout the ventricles. To some extent, an interpretation of an equivalent electric heart axis based on solid angle theory [22] could help to understand the source of disagreement. The electric heart axis is determined when the R-wave appears in the ECG waveform recorded from

the body surface. The question is whether the depolarization propagation is advanced for each examined subject, in respect to the geometry of the ventricles, to the same extent. In general, a precise estimation of the electrical axis of the heart using a limited number of electrodes is a challenging task. It could be shown that for a measurement lead consisting only of two electrodes the dipole translation in 3D space is indistinguishable from its rotation. The electrical heart axis is estimated by measuring its components, i.e. by measuring the voltage between electrodes appropriately attached to the thorax. Thus, other factors, aside from the source of the potential (i.e. the dipole), influencing its distribution should be considered, too.

V. CONCLUSION

QRS morphology-based EDR signal depends on many factors, among them on respiration-induced changes of lungs' conductivity and heart movement (rotation and translation). The heart rotation and translation seem to be dominating mechanisms. The mechanisms themselves and the relationship between them are subject-dependent and such are their contributions to EDR signal. This allows to explain the inter-subject variability of the parameters describing the EDR signal to which selected parameters of the QRS complex are used, e.g. the R-wave amplitude. The quality of the respiratory signal obtained on the basis of the variability of the selected QRS complex parameter depends on the geometrical relationship of the electrocardiographic lead used and changes in the position and direction of the heart's electrical vector. This does not allow, a priori, to select a lead configuration that allows to obtain the EDR signal with the maximum amplitude. Including the heart translation to the set of mechanisms influencing the EDR signal enables explanation of its phase shift in relation to the nasal airflow signal. Recommendation the EDR method for a certain application, e.g. monitoring respiration activity during sleep, demands further studies. Nevertheless, the achieved results allow to develop both methods and equipment for wearable and monitoring devices while maintaining or even reducing the complexity of measurement systems construction.

REFERENCES

[1] P. De Chazal, C. Heneghan, E. Sheridan, R. Reilly, P. Nolan, and M. O'Malley, "Automated processing of the single-lead electrocardiogram for the detection of obstructive sleep apnoea," *IEEE Trans. Biomed. Eng.*, vol. 50, no. 6, pp. 686–696, Jun. 2003.

[2] P. Przystup, A. Bujnowski, J. Rumiński, and J. Wtorek, "A detector of sleep disorders for using at home," *J. Telecommun. Inf. Technol.*, no. 2, pp. 70–78, 2014.

[3] M. Tobin, "Breathing pattern analysis," *Intensive Care Med.*, vol. 18, no. 4, pp. 193–201, 1992.

[4] S. C. Tarrant, R. E. Ellis, F. C. Flack, and W. G. Selley, "Comparative review of techniques for recording respiratory events at rest and during deglutition," *Dysphagia*, vol. 12, no. 1, pp. 24–38, 1997.

[5] R. Bailón, L. Sörnmo, and P. Laguna, "ECG-derived respiratory frequency estimation," in *Advance Methods Tools for ECG Data Analysis*. Norwood, MA, USA: Artech House, 2006, ch. 8, pp. 215–244.

[6] E. Helfenbein, R. Firoozabadi, S. Chien, E. Carlson, and S. Babaeizadeh, "Development of three methods for extracting respiration from the surface ECG: A review," *J. Electrocardiol.*, vol. 47, no. 6, pp. 819–825, 2014.

[7] I. Hagerman, J. Nowak, J. Svedenhag, O. Nyquist, and C. Sylvén, "Beat-to-beat QRS amplitude variability during dobutamine infusion in patients with coronary artery disease," *Cardiology*, vol. 87, no. 2, pp. 161–168, 1996.

[8] P. Przystup, A. Poliński, A. Bujnowski, T. Kocejko, and J. Wtorek, "A body position influence on ECG derived respiration," in *Proc. 39th Annu. Int. Conf. Eng. Med. Biol. Soc. (EMBC)*, Sep. 2017, pp. 3513–3516.

[9] H. Riekkinen and P. Rautaharju, "Body position, electrode level, and respiration effects on the Frank lead electrocardiogram," *Circulation*, vol. 53, no. 1, pp. 40–45, 1976.

[10] G. G. Berntson, J. T. Cacioppo, and K. S. Quigley, "Respiratory sinus arrhythmia: Autonomic origins, physiological mechanisms, and psychophysiological implications," *Psychophysiology*, vol. 30, no. 2, pp. 183–196, 1993.

[11] H. L. Chan, S. H. Lin, F. T. Wang, W. Y. Hsu, and C. L. Wang, "ECG-derived respirations based on phase-space reconstruction of single-lead ECG: Validations over various physical activities based on parallel recordings of ECG, respiration, and body accelerations," in *Proc. 36th Annu. Int. Conf. Eng. Med. Biol. Soc. (EMBC)*, Aug. 2014, pp. 2282–2285.

[12] P. W. Macfarlane, A. Van Oosterom, O. Pahlm, P. Kligfield, M. Janse, and J. Camm, *Comprehensive Electrocardiology*. New York, NY, USA: Springer, 2010.

[13] G. D. Furman, Z. Shinar, A. Baharav, and S. Akselrod, "Electrocardiogram derived respiration during sleep," *Comput. Cardiol.*, vol. 32, pp. 351–354, Sep. 2005.

[14] B. Pilgram and M. Di Rienzo, "Estimating respiratory rate from instantaneous frequencies of long team heart rate tracings," *Comput. Cardiol.*, vol. 20, pp. 859–862, Sep. 1993.

[15] R. Pallas-Areny, J. Colominas-Balague, and F. J. Rosell, "The effect of respiration-induced heart movements on the ECG," *IEEE Trans. Biomed. Eng.*, vol. 36, no. 6, pp. 585–590, 1989.

[16] A. Travaglini, C. Lamberti, J. DeBie, and M. Ferri, "Respiratory signal derived from eight-lead ECG," *Comput. Cardiol.*, vol. 25, pp. 65–68, Sep. 1998.

[17] M. Varanini, G. De Paolis, M. Emdin, A. Macerata, S. Pola, M. Cipriani, and C. Marchesi, "Spectral analysis of cardiovascular time series by the S-transform," *Comput. Cardiol.*, vol. 24, pp. 383–386, Sep. 1997.

[18] G. B. Moody, R. G. Mark, A. Zoccola, and S. Mantero, "Derivation of respiratory signals from multi-lead ECGs," *Comput. Cardiol.*, vol. 12, pp. 113–116, Oct. 1985.

[19] D. Widjaja, J. C. V. Perez, A. C. Dorado, and S. Van Huffel, "An improved ECG-derived respiration method using kernel principal component analysis," *Comput. Cardiol.*, vol. 38, pp. 45–48, Sep. 2011.

[20] K. Ramya and K. Rajkumar, "Respiration rate diagnosis using single lead ECG in real time," *Global J. Med. Res.*, vol. 13, no. 1, 2013. [Online]. Available: https://www.medicalresearchjournal.org/index.php/GJMR/article/view/315

[21] D. B. Geselowitz, "On bioelectric potentials in an inhomogeneous vol. conductor," *Biophys. J.*, vol. 7, no. 1, pp. 1–11, 1967.

[22] J. Malmivuo and R. Plonsey, *Bioelectromagnetism: Principles and Applications of Bioelectric and Biomagnetic Fields*. Oxford, U.K.: Oxford Univ. Press, 1995.

[23] T. Kokki, R. Klén, T. Noponen, and J. Pärkkä, "Linear relation between spirometric vol. and, the motion of cardiac structures: MRI and clinical PET study," *J. Nucl. Cardiol.*, vol. 23, no. 3, pp. 475–485, 2016.

[24] G. Shechter, C. Ozturk, J. R. Resar, and E. R. McVeigh, "Respiratory motion of the heart from free breathing coronary angiograms," *IEEE Trans. Med. Imag.*, vol. 23, no. 8, pp. 1046–1056, Aug. 2004.

[25] A. E. Holland, J. W. Goldfarb, and R. R. Edelman, "Diaphragmatic and cardiac motion during suspended breathing: Preliminary experience and implications for breath-hold MR imaging," *Radiology*, vol. 209, no. 2, pp. 483–489, 1998.

[26] R. M. Gulrajani, "The forward problem of electrocardiography: Theoretical underpinnings and applications," in *Modeling Imaging Bioelectrical Activity*. London, U.K.: Springer, 2004, ch. 2, pp. 43–79.

[27] A. V. Shahidi and P. Savard, "Forward problem of electrocardiography: Construction of human torso models and field calculations using finite element method," *Med. Biol. Eng. Comput.*, vol. 32, no. 1, pp. S25–S33, 1994.

[28] R. N. Klepfer, C. R. Johnson, and R. S. MacLeod, "The effects of inhomogeneities and anisotropies on electrocardiographic fields: A 3-D finite-element study," *IEEE Trans. Biomed. Eng.*, vol. 44, no. 8, pp. 706–719, Aug. 1997.

[29] L. Bear, L. Cheng, I. LeGrice, and G. Sands, "Forward problem of electrocardiography: Is it solved?" *Circulat., Arrhythmia Electrophysiol.*, vol. 8, no. 3, pp. 677–684, 2015.

[30] C. P. Bradley, A. J. Pullan, and P. J. Hunter, "Effects of material properties and geometry on electrocardiographic forward simulations," *Ann. Biomed. Eng.*, vol. 28, no. 7, pp. 721–741, 2000.

[31] Y. Rudy, "The forward problem of electrocardiography revisited," *Circulat., Arrhythmia Electrophysiol.*, vol. 8, no. 3, pp. 526–528, 2015.

[32] Y. Rudy, R. Plonsey, and J. Liebman, "The effects of variations in conductivity and geometrical parameters on the electrocardiogram, using an eccentric spheres model," *Circulat. Res.*, vol. 44, no. 1, pp. 104–111, 1979.

[33] D. Gabor and C. Nelson, "Determination of the resultant dipole of the heart from measurements on the body surface," *J. Appl. Phys.*, vol. 25, no. 4, pp. 413–416, 1954.

[34] D. B. Geselowitz, "On the theory of the electrocardiogram," *Proc. IEEE*, vol. 77, no. 6, pp. 857–876, Jun. 1989.

[35] R. M. Gulrajani, "The forward and inverse problems of electrocardiography," *IEEE Eng. Med. Biol. Mag.*, vol. 17, no. 5, pp. 84–101, 122, Sep. 1998.

[36] R. Plonsey and R. C. Barr, *Bioelectricity: A Quantitative Approach*. New York, NY, USA: Springer, 2007.

[37] S. Gratiy, G. Halnes, and D. Denman, "From Maxwell's equations to the theory of current-source density analysis," *Eur. J. Neurosci.*, vol. 45, no. 8, pp. 1013–1023, 2017.

[38] C. Nelson, B. Hodgkin, and P. Gastonguay, "Dipole moment of the hearts of various species," *Ann. Biomed. Eng.*, vol. 3, no. 3, pp. 308–314, 1975.

[39] J. Wtorek, "Relations between components of impedance cardiogram analyzed by means of finite element model and sensitivity theorem," *Ann. Biomed. Eng.*, vol. 28, no. 11, pp. 1352–1361, 2000.

[40] C. Gabriel, A. Peyman, and E. H. Grant, "Electrical conductivity of tissue at frequencies below 1 MHz," *Phys. Med. Biol.*, vol. 54, no. 16, p. 4863, 2009.

[41] S. Gabriel, R. W. Lau, and C. Gabriel, "The dielectric properties of biological tissues: II. Measurements in the frequency range 10 Hz to 20 GHz," *Phys. Med. Biol.*, vol. 41, no. 11, p. 2251, Nov. 1996.

[42] J. Wtorek, L. Jozefiak, A. Polinski, and J. Siebert, "An averaging two-electrode probe for monitoring changes in myocardial conductivity evoked by ischemia," *IEEE Trans. Biomed. Eng.*, vol. 49, no. 3, pp. 240–246, Mar. 2002.

[43] J. Wtorek and A. Polinski, "The contribution of blood-flow-induced conductivity changes to measured impedance," *IEEE Trans. Biomed. Eng.*, vol. 52, no. 1, pp. 41–49, Jan. 2005.

[44] H. P. Schwan and S. Takashima, "Dielectric behavior of biological cells and membranes (commemoration issue dedicated to professor Tetsuya Hanai on the occasion of his retirement)," *Bull. Inst. for Chem. Res.*, vol. 69, no. 4, pp. 459–475, 1991.

[45] J. Zhang and R. Patterson, "Non-invasive determination of absolute lung resistivity in adults using electrical impedance tomography," *Physiol. Meas.*, vol. 31, no. 8, pp. S45–S56, 2010.

[46] M. Ragnarsdóttir and E. Kristinsdottir, "Breathing movements and breathing patterns among healthy men and women 20–69 years of age," *Respiration*, vol. 73, no. 1, pp. 48–54, 2006.

[47] C. G. Xanthis, P. Bonovas, and G. A. Kyriacou, "Inverse problem of ECG for different equivalent cardiac sources," *Piers*, vol. 3, no. 8, pp. 1222–1227, 2007.

[48] F. Yang and R. P. Patterson, "A simulation study on the effect of thoracic conductivity inhomogeneities on sensitivity distributions," *Ann. Biomed. Eng.*, vol. 36, no. 5, pp. 762–768, May 2008.

[49] N. Okamoto, K. Kaneko, E. Simonson, and O. Schmitt, "Reliability of individual frontal plane axis determination," *Circulation*, vol. 44, no. 2, pp. 213–219, 1971.

[50] H. Engblom, J. Foster, T. Martin, and B. Groenning, "The relationship between electrical axis by 12-lead electrocardiogram and anatomical axis of the heart by cardiac magnetic resonance in healthy subjects," *Amer. Heart J.*, vol. 150, no. 3, pp. 507–512, 2005.

PIOTR PRZYSTUP received the M.Sc. degree in electronics from the Gdańsk University of Technology, Poland, in 2012. After that, he started Ph.D. studies with the Biomedical Engineering Department, Gdańsk University of Technology.

He worked several years as a Hardware Designer. He is currently the CEO of Dynamic Precision in Gdańsk, Poland—design office providing electronic designs for military, industrial, automotive and medical applications, and the CEO in DP IOT in Gdańsk—company focused on Internet of Things solutions. His current research interests include ECG signal mechanisms and their influence on other biosignals.

ARTUR POLIŃSKI received the M.S. degree in electronics from the Gdańsk University of Technology, Gdańsk, Poland, in 1994, the M.S. degree in mathematics from the University of Gdańsk, Gdańsk, in 1997, the Ph.D. degree in electronics from the Gdańsk University of Technology, in 1999, and the Ph.D. degree in mathematics from the University of Gdańsk, in 2007.

His research interests include the development of noninvasive methods for the assessment of cardiovascular systems, biomedical signal analysis and processing, and modeling and simulations of the diagnostic methods.

JERZY WTOREK received the M.S., Ph.D., and D.Sc. degrees in electronics and biomedical engineering from the Gdańsk University of Technology, Poland, in 1976, 1986, and 2004, respectively. He was an Assistant Professor, from 1976 to 1986, an Assistant Professor, from 1987 to 2003, and an Associate Professor, from 2004 to 2016. Since 2016, he has been a Professor with the Gdańsk University of Technology. His research interests include the development of noninvasive methods for the assessment of cardiovascular systems, tissue immitance properties, and impedance spectroscopy.

He is a member of the Polish Biomedical Engineering Society and the Polish Society of Medical Physics.

• • •